

1 **A morphological classification of coastal forelands, with examples from South Africa**

2

3 Jasper Knight^{1*}, Helene Burningham²

4 ¹School of Geography, Archaeology & Environmental Studies, University of the

5 Witwatersrand, Johannesburg 2050, South Africa

6 ²Department of Geography, UCL, Gower Street, London WC1E 6BT, UK

7 *Author for correspondence: jasper.knight@wits.ac.za

8

9 **Abstract**

10 Alongshore variations in the cross-shore width, and therefore volume, of sandy beaches are
11 important because these reflect spatial variability in the operation of wave- and wind-driven
12 processes taking place both at the shoreface and in the supratidal zone. One key geomorphic
13 signature of variations in cross-shore beach width is the development of coastal forelands.
14 Different foreland types have been described in the literature from very specific geomorphic
15 contexts, but hitherto there has been no overarching classification scheme that genetically
16 links these different foreland types, or considers them in the wider context of sandy beach
17 dynamics. In order to achieve this aim, this study maps and inventorises 87 forelands from
18 the South African coast (~2600 km long), and classifies these into four morphological types:
19 salients, tombolos, cusped forelands, and ramp forelands. These foreland types have different
20 morphological properties, reflecting the interplay of coastal erosional and depositional
21 processes and any antecedent conditions; and a varying balance of morphodynamic controls
22 on their development and behaviour. These include variations in wave (and to a lesser extent
23 wind) energy, sediment supply, and the presence of bedrock outcrops of different sizes,
24 shapes and positions along the shoreline. Analysis of foreland morphology and dynamic
25 behaviour, based on examples from South Africa, enables a better understanding of coastal

26 forelands globally as integrated sediment systems and responsive to the range of forcings
27 driving coastal change.

28

29 **Keywords:** Coastal dynamics; Forelands; Headland bypass systems; Longshore processes;
30 Supratidal zone; Wave processes

31

32 **Introduction**

33 Longshore and cross-shore variations in sandy coast sediment budgets result in, amongst
34 other outcomes, changes in beach width, width of the intertidal, supratidal and shoreface
35 elements of beaches, and development of distinctive sedimentary landforms (Sanderson et al.,
36 2000). This dynamic behaviour of sandy beaches is achieved mainly through wave and wind
37 process regimes, and also influenced by longshore currents, tides, incoming rivers, and
38 headland bypass systems (Boeyinga et al., 2010; Goodwin et al., 2013; Vieira da Silva et al.,
39 2018). One key geomorphic expression of this alongshore variation in cross-shore sediment
40 accumulation is the *coastal foreland*. Forelands are shoreline protuberances formed by the
41 seaward progradation of the littoral shoreline, often mirrored by backshore accommodation of
42 dunes and/or beach ridges, along a certain coastal stretch. This development takes place as a
43 combination of wave and current processes to form ‘promontories of the mainland’, to use
44 Gulliver’s (1896, p.400) original definition. The most well-known foreland type reported in
45 the literature is the cusped foreland. This develops where shoreline progradation takes place
46 in the form of nested gravel beach ridges that have a consistent alignment at an oblique angle
47 to the shore (e.g., Semeniuk et al., 1988; McNinch and Leuttich, 2000; Alcántara-Carrió and
48 Fontán, 2009). Cusped forelands thus have a regular progradational character controlled by
49 the linear and nested nature of these beach ridges (Carter, 1980; Fontolan and Simeoni, 1999;
50 Roberts and Plater, 2007; Lampe and Lampe, 2018) and driven by differential wave action

51 (Falqués et al., 2018). These forelands therefore develop a distinctive triangular-shaped
52 morphology with generally symmetrical lateral margins, and may have backbarrier lagoons or
53 wetlands behind the foreland or between individual beach ridges within the foreland itself.
54 Cuspate forelands exhibiting these general characteristics are noted in particular along the
55 glaciated northwest Europe and northeast North America coasts (Long and Hughes, 1995;
56 Roberts and Plater, 2007; Clemmensen et al., 2011; Xhardé et al., 2011; St-Hilaire-Gravel et
57 al., 2015; Hesp et al., 2016) and this foreland type can thus be classified as a paraglacial
58 landform linked to the deposition of gravel beach ridges from glacial sediment sources
59 during phases of sea-level change. Cuspate forelands can be considered as accommodation-
60 limited systems controlled by longshore processes along the foreland margins. Other cuspate
61 forelands, however, can be considered as sediment-limited systems where sediment is stored
62 on nearshore shoals and where waves, and to a lesser extent tides and fluvial pumping, drive
63 seasonal onshore sediment transport to the foreland apex (McNinch and Luettich, 2000; Park
64 and Wells, 2005, 2007; Kumar et al., 2013).

65

66 Despite this historical emphasis in the literature on cuspate forelands, similar progradational
67 morphologies are also found along sandy coasts (Fig. 1). These include tombolos and salients
68 that develop as a result of wave refraction around offshore islands or reefs (Semeniuk et al.,
69 1988; Sanderson and Eliot, 1996; Sanderson et al., 2000; Black et al., 2020; de Macêdo et al.,
70 2022), and ramp forelands (defined in this study) that develop where wave- and wind-
71 deposited sediments prograde across a low-elevation bedrock surface. Therefore, coastal
72 forelands (*sensu lato* and as defined below) are part of a continuum of sandy coastal beach
73 morphologies that reflect the interplay among sediment availability, the presence of bedrock
74 outcrops or protuberances, and different forcing factors (waves, sediment supply, sea-level
75 trajectory) that can result in long- to short-term patterns of differential coastal aggradation or

76 erosion along any coastal stretch (Heron et al., 1984; Sanderson et al., 2000; Falqués et al.,
77 2018; Orlando et al., 2019; Gallop et al., 2020). Because of the presence of these
78 morphological types along a continuum of forms, the non-genetic term *coastal foreland* is
79 used in this study for all foreland types. Coastal forelands are defined herein as *a prominent*
80 *and persistent (decadal-scale) protrusion of a littoral shoreline in response to the differential*
81 *action of wave erosion and deposition processes*. This is a broader yet more precise definition
82 than the encyclopaedia definition given by Craig-Smith (2005). The broad structure of all
83 types of forelands as defined in this study, including their key associated geomorphic
84 elements in plan form and cross profile, is shown in Figure 1.

85
86 Because there are limitations of the currently narrow definition and understanding of
87 forelands, the main aim of this study is to propose a typology of sandy coastal forelands
88 (*sensu lato*) applicable globally, based on examples observed along the South African coast
89 (~2600 km long). This study is unique for three reasons: (1) it proposes an integrated global
90 classification for coastal foreland types (Fig. 1) that considers them as a morphological
91 continuum of forms and not as simple evolutionary endmembers. This has not been achieved
92 before; (2) no previous study has mapped and classified coastal forelands at a national scale;
93 and (3) this is the first study that examines these landform types in South Africa (or indeed in
94 Africa).

95
96 In detail this paper (1) maps the distribution and properties of forelands along the South
97 African coast in order to distinguish and classify the forelands into different morphological
98 types; (2) describes the morphodynamics and properties of the foreland types; and (3)
99 proposes an evolutionary model for coastal foreland systems that focuses on the sediment
100 dynamics that contribute to their development. The foreland classification scheme presented

101 in this study can be usefully applied to sandy coasts globally, and represents a significant
102 advance in how longshore variations in the width of these sedimentary accumulations can be
103 conceptualised. This is particularly important given the sensitivity of sandy coasts to climate
104 forcing (Knight and Harrison, 2009; Luijendijk et al., 2018) and thus the role of sandy
105 beaches as a buffer to the effects of storm waves and ongoing sea-level rise (Nordstrom and
106 Terich, 1986; Dolphin et al., 2007, 2011; Orlando et al., 2019).

107

108 **Study area**

109 The geomorphology of the South African coast has only been examined at a regional scale
110 (Tinley, 1985; Dardis and Grindley, 1988) and thus there is still much information lacking
111 about its detailed coastal landforms and their dynamics. Long and uninterrupted sandy coasts
112 are present on different sectors of the South African coast, and exposed to different prevailing
113 wind and wave climates (Mitchell et al., 2005) (Fig. 2). The nature of these coastal sediment
114 systems varies significantly. Laterally extensive sandy beaches have a consistent width,
115 backed variably by unvegetated transverse dune complexes, and exhibit a sharp and often
116 linear landward boundary that is marked by vegetated foredunes. Along the southeast-facing
117 coastline of South Africa in particular, sandy beaches are dissected by small perennial rivers
118 that result in the formation of microtidal estuaries (Cooper, 2001; Bate et al., 2017). Along all
119 coastal sectors, sandy beaches including pocket beaches may be constrained by bedrock
120 headlands that influence the size and shape of sediment cells (Tinley, 1985; Meeuwis and van
121 Rensburg, 1986; Dardis and Grindley, 1988). There are spatial differences in external forcing
122 by wind, waves and tides between the south/east (Indian Ocean) and west (Atlantic) coasts in
123 South Africa (Corbella and Stretch, 2012a; Rautenbach et al., 2019; Veitch et al., 2019).
124 Winds are predominantly shore-parallel along all coastal sectors (Schumann and Martin,
125 1991). Tides are semi-diurnal and high microtidal/low mesotidal (range ~2.0–2.5 m) with a

126 non-residual component that increases from west to east (Searson, 1994). Waves ($H_s > 5$ m;
127 Corbella and Stretch, 2012c; Wepener and Degger, 2019) exert a significant forcing on
128 shoreline dynamics in South Africa (Corbella and Stretch, 2012a, b). Despite this
129 background, there have been relatively few studies on beach morphodynamics and the
130 sensitivity and responses of beach systems to storm and wave forcing (Harris et al., 2011;
131 Corbella and Stretch, 2012a, b; Guastella and Smith, 2014; Green et al., 2019). More
132 frequently there have been studies that examine the dynamics of coastal sediment systems,
133 especially dune–beach systems (La Cock et al., 1992; Olivier and Garland, 2003; Mitchell et
134 al., 2005; Knight and Burningham, 2021) and headland–embayment systems (Meeuwis and
135 van Rensburg, 1986), but these specific and localised case studies have not been compared to
136 each other or integrated into a wider coastal sediment systems model.

137

138 **Methods**

139 In order to map and identify the large-scale properties of coastal forelands in South Africa,
140 the country’s coastline was systematically examined using Google Earth imagery. This is
141 similar to methodologies used in other studies of coastal forelands, including assessing their
142 changes over time (e.g., Kunte and Wagle, 1993; Clemmensen et al., 2011; Xhardé et al.,
143 2011; Allen et al., 2012; Hesp et al., 2016). In this coastal survey, the locations and general
144 geomorphic properties of individual forelands were identified and then digitised from the
145 most recent (2020) Google Earth imagery, and key metrics calculated were *length*, *width*,
146 *area* and *skewness* of the foreland. *Length* (in m) is defined as the alongshore distance
147 between the up- and down-drift limits of any single foreland system. These limits, essentially
148 representing the sediment closure width of that foreland system, are located where the beach
149 is narrowest which often coincides with the position of (ephemeral or perennial) river mouths
150 (Fig. 3a) or rocky headlands. These act as barriers to continuous longshore sediment transport

151 and thus their positions along the shoreline can be used to compartmentalise the relatively
152 continuous beach systems. *Width* refers to the maximum seaward extent (in m) of the sandy
153 foreland at its apex point, as measured perpendicular to the landward boundary between the
154 beach and the vegetated dunes. Commonly the foreland apex is anchored on a bedrock
155 outcrop. *Area* is calculated as the area (in m²) enclosed within the digitised polygon of the
156 outer margin of the foreland, which includes its longshore limits, and the landward and
157 seaward extents of the functional (dynamical) components of the forelands, thus excluding
158 thickly vegetated dunes for example. Axial *skewness* or asymmetry of the foreland refers to
159 the position, along its length, of the greatest foreland width (apex point). If the greatest width
160 is located half way along the length, like an isosceles triangle, then the foreland is broadly
161 symmetric. If the greatest width is located nearer to the up- or down-drift limits, like a
162 scalene triangle, then the foreland is asymmetric or skewed in a certain longshore direction
163 (Fig. 3b, c). ‘Foreland activity’ identified in Table 1 is a generalised qualitative evaluation of
164 the foreshore, shoreline, and backshore dynamics of each foreland based on a simple visual
165 comparison of recent (last 5 years) Google Earth images. If the shorelines of each foreland
166 vary significantly over this timeframe the foreland is classified as *active*; if they appear static
167 the foreland is *inactive*; and if they vary only to some extent the foreland is classified as
168 *partly active*. A more rigorous quantitative evaluation of foreland dynamics was not
169 undertaken in this study.

170

171 After identification as described above, the forelands were systematically examined for the
172 presence of key geomorphic features including the presence and properties of transverse,
173 fixed (contemporary, vegetated), and ramp dunes (cf., Carter and Wilson, 1993); any smaller
174 aeolian depositional forms such as minor humps and undulations in the supratidal zone;
175 bedrock outcrops within the varied sediment accumulations; any vegetated and inactive dunes

176 at the back of the beach; evidence for erosional or progradational features of the beach
177 shoreface; and the presence of absence of a river mouth as a significant sediment source. In
178 addition to the previously described foreland morphometrics, the length of bedrock along the
179 foreland shoreline was calculated as a proportion of the total foreland length. In combination,
180 a principal component analysis (PCA) was then undertaken to explore the parameter space
181 (feature presence/absence was presented as binary measures) and establish key gradients
182 across the multiple variables. The program PAST (Hammer et al., 2001) was used for this
183 purpose to calculate the eigenvalues of the correlation matrix. The first two principal
184 components captured 34% of the total variance in the parameters used here to describe
185 foreland morphology.

186

187 **Results**

188 *Distribution and properties of forelands along the South African coast*

189 In total, 87 forelands are identified along the South African coast (Fig. 4). Their key
190 geomorphic characteristics are shown in Table 1. Forelands are found mainly along sand-
191 dominated stretches of the coastline where sediment supply is greatest, but are also found
192 along predominantly rocky stretches where sediment accumulates around river mouths. Four
193 different foreland types are identified (Fig. 1).

194

195 *Foreland type 1 – salient.* This is formed where wave refraction takes place around an
196 offshore bedrock island or reef, resulting in enhanced seaward sediment deposition in the
197 wake of the reef. In this study four salients were identified (5% of all forelands), three of
198 which are on the west coast (Fig. 4).

199

200 *Foreland type 2 – tombolo*. This most commonly forms by initial development of a salient,
201 where an offshore island that forces wave refraction becomes linked to the mainland by the
202 continued accumulation of wave-transported sediment. In this study nine tombolos were
203 identified (10% of all forelands) (Fig. 4).

204

205 *Foreland type 3 – cusate foreland*. This is a distinctive triangular-shaped foreland formed by
206 longshore processes, driven by wave erosion and sediment transport on the two sides of the
207 foreland. Classically, cusate forelands show the development of nested parallel beach ridges
208 that are commonly overlain by sand dunes (high sand sediment supply), which may contain
209 wetlands in ridge swales (low sediment supply or gravel-dominated systems). In this study 46
210 cusate forelands were identified (Fig. 4), making them the most common foreland type
211 (53% of the total) (Table 1). Cusate forelands often reflect local alongshore sediment
212 transport patterns and may be symmetric in plan view, or asymmetric (skewed). Of these
213 forelands, 21 (46%) are symmetric, 21 (46%) are skewed to the north and only four (9%) are
214 skewed to the south. Of the four cusate forelands along the south coast, two are symmetric
215 and two are skewed to the east.

216

217 *Foreland type 4 – ramp foreland*. This landform is specifically named and described in this
218 study for the first time. Ramp forelands occur where sand covers the surface of a low-
219 elevation bedrock platform, allowing the beach to extend farther seaward. In a longshore
220 direction, sediment thins as it rises up the bedrock ramp surface to the top of the foreland,
221 which corresponds to the location of its maximum width, and then thickens down the leeside.
222 Ramp forelands are therefore distinct from cusate forelands (*sensu stricto*) in the elevated
223 nature of the bedrock bench or shelf that raises the supratidal deposits above the tidal frame.
224 In this study 28 ramp forelands were identified (32% of all forelands) and these are mainly

225 located on the south and east coasts (Fig. 4). Considering all the ramp forelands, five (18%)
226 are symmetric whereas of those that are skewed, the majority (20 of 23) are skewed to the
227 north with only a few (3 of 23) to the south. Of the five ramp forelands on the south coast,
228 four are skewed to the east, and one to the west.

229

230 The key morphometric properties of all 87 forelands (of all types) identified in this study are
231 illustrated spatially in Figure 5. There are no systematic spatial (alongshore) patterns in
232 foreland properties between different coastlines. Comparison of the generalised morphometry
233 of the four foreland types is given in Figure 6. There is less variability in foreland width than
234 there is in length. Cuspate forelands are the largest landforms and several of these are
235 significant landforms in terms of their length and area, with nine of the ten forelands over 2
236 million m² (200 ha) in area being cuspate forelands (Table 1). This may suggest that cuspate
237 forelands, by virtue of their size, have different morphodynamic behaviours to other foreland
238 types. Salients are largely near-symmetrical, whilst ramp forelands are more significantly
239 skewed because they reflect longshore processes and alongshore winds. Both cuspate and
240 ramp forelands are more elongated (larger length relative to width) in comparison to salients
241 and tombolos, which are more equidimensional. Forelands comprise a range of bedrock
242 shoreline controls, with cuspate and ramp forelands tending to have the potential for greater
243 extents of bedrock shorelines compared to salients and tombolos. Comparison of some of
244 these morphometric factors in a geographical context suggests that west coast forelands are
245 more compact (have somewhat higher width/length values; Fig. 5) than east coast forelands
246 (average of 0.261 compared to 0.190, respectively), which may reflect the more vigorous
247 wave regime and lower sediment availability.

248

249 Some specific examples illustrate the properties of these forelands. The salient at
250 Visagiesfontein (#1 on Table 1 and Fig. 4) (Fig. 7a) is developed at around 100 m distance in
251 the lee of a bedrock outcrop and is broadly symmetric in plan view but with a slight
252 southward skew. Observation over multiple time periods (in Google Earth) shows waves to
253 be shore parallel, suggesting that the salient is morphodynamically at equilibrium with
254 respect to wave regime. The surface of the salient is relatively flat, with no supratidal dune
255 development. A notable feature at this site is evidence for sand mining on the coastal plain
256 behind the salient. Borrow pits are visible at the north end and at the apex of the salient (3
257 February 2016), but these pits have disappeared in the subsequent image (24 November
258 2018). Further, the stable morphology of the salient suggests that sand mining has not
259 affected its morphodynamics over recent last decades.

260

261 The tombolo at Robberg (#26) (Fig. 7b) is connected to an offshore island comprised of
262 aeolianite. This aeolianite was dated by Carr et al. (2019) using the luminescence method to
263 the period ~35–41 ka (middle of marine isotope stage (MIS) 3), suggesting that today's
264 tombolo developed in response to progressive marine erosion and development of this island
265 as a topographic feature, in the post-MIS 3 period. Aeolianite on this island and on the
266 landward Robberg peninsula have helped anchor this system, and force refraction, with
267 tombolo sediment provided by reworking of recent dunes in the centre of the peninsula, or
268 where tombolo surface sediments are blown inland into this dune system (Hellström and
269 Lubke, 1993). The width of the tombolo appears to vary seasonally, narrowing on both sides
270 in the winter as likely result of bigger waves. The shoreface around the tombolo margins is
271 steep and sharp-crested.

272

273 The cusplate foreland at Oceana Beach (#39) (Fig. 7c) is asymmetric and anchored on a broad
274 intertidal shore platform. This is defined as a cusplate foreland because sediment availability
275 does not vary along the length of the foreland, in contrast to ramp forelands where sediment
276 thins up the bedrock ramp. The ramp foreland at Fort D’Acre (#42) (Fig. 7d) has a broader
277 shoreface than the cusplate forelands.

278

279 The PCA results of morphometric and geomorphic analysis of each of the forelands identified
280 (Table 1) are shown in Figure 8. The results show that there is wide variability in the
281 composition, structure and size of the contemporary forelands along this coast. The PCA
282 allows six morphometric form types to be identified – these are labelled types a–f on Figure 8
283 and correspond to the morphological continuum between cusplate and ramp foreland types
284 (mostly types b and c, respectively). Tombolos and salients are not resolved as discrete
285 morphotypes in Figure 8, but are mainly represented by type e. In total, around one third of
286 the total variance is captured by the parameters of foreland size, the presence and absence of
287 specific aeolian forms, and the role of rock within the foreland. Larger forelands (types a–c)
288 generally comprise significant areas of unvegetated transverse dunes, backed in many cases
289 by densely vegetated and inactive (fossilised) dunes (see Knight, 2021), and their shape is
290 notably skewed in an alongshore down-drift direction. These foreland types are all found on
291 the east coast, and can be secondarily differentiated by the presence of bedrock close to, or
292 protruding above, the contemporary aeolian surface. A wider range of forelands are found
293 across all shorelines, and these are more generally characterised as more compact and
294 symmetrical forms (types d–f) and are found mainly along the west coast. Some relate to
295 significantly rocky shorelines, and exist as unvegetated, small aeolian deposits at the rear of
296 the beach. With reduced dominance of rock along the shoreline, the forelands are generally
297 more vegetated, but are further distinguished by the presence or absence of erosional features

298 such as deflation hollows. A smaller group of forelands is differentiated by the presence of
299 specific progradational forms such as beach ridges; bedrock is still evident within the
300 nearshore zone, but these are the closest geomorphologically to cusped forelands. Specific
301 examples of form types a–f are presented in Figure 9. These illustrate schematically the main
302 geomorphic elements of these types that allow them to be distinguished from each other, and
303 therefore why they plot in different areas of the PCA.

304

305 Although there is a broad association of forelands with sandy coastal stretches (Fig. 4) there
306 is essentially a random pattern of foreland size and shape over space despite closely located
307 forelands commonly having similar properties (Fig. 5). This appears true for both north–south
308 oriented coastlines (along the west and east coasts), and the west–east oriented coastline
309 along the southern Cape coast. In addition, the different foreland types are found along all
310 sectors of the coast apart from the limited number of salient found mainly along the west
311 coast. There is a clustering of forelands along the Eastern Cape and northern KwaZulu-Natal
312 coasts of South Africa, with densities of <16 forelands/100 km.

313

314 Of note here is that both cusped and ramp foreland types have well developed transverse
315 dunes (defined by Hunter et al., 1983) within the supratidal zone (e.g., Knight and
316 Burningham, 2019, 2021; Jackson et al., 2020). Erosion of the vegetated dunes to the rear of
317 these forelands is evidenced by the ragged dune edge and shows that sediment can be
318 transferred from the dunes to the beach, and *vice versa*. It is also notable that over time the
319 margins of these foreland systems are stable with a continuous shoreface, suggesting they are
320 largely at equilibrium with respect to wave forcing (but this is discussed below).

321

322 **Discussion**

323 Forelands can be considered as locations along extensive sandy coastlines where sediments
324 show net accumulation leading to seaward progradation and therefore development of the
325 foreland shape. Forelands are shown here to be relatively common, but underreported,
326 landforms along the South Africa coast, and are located along both sand-dominated and rock-
327 dominated coastal stretches (Figs. 2, 4). Sand-dominated stretches have generally linear and
328 narrow sandy beaches with well-vegetated backing dunes (Tinley, 1985; Dardis and
329 Grindley, 1988). Along the east coast where a narrow shelf and steep coastal hinterland is
330 usually present, forelands are found particularly in association with river mouths (Table 1)
331 where sediment supply overwhelms the limited accommodation space. It is notable that the
332 sand-dominated west (Atlantic) coast contains significantly fewer forelands in total and by
333 density per 100 km (values of 2 to 4) compared to much higher values (5 to 16/100 km) along
334 the east (Indian) coast. However, the west coast contains most of the (4) salients identified in
335 this study, which is indicative of high wave energy conditions (Sanderson and Eliot, 1996).
336 The role of wave energy in shaping the lateral margins of forelands as well as supplying
337 longshore sediment to the foreland apex is well established (Carter, 1980; Heron et al., 1984;
338 Ashton et al., 2001). Seasonal changes in wave direction and height can lead to beach rotation
339 (Dolphin et al., 2011), asymmetric foreland shapes (Sanderson et al., 2000) and formation of
340 ‘travelling forelands’ where the entire foreland shape migrates alongshore (Escoffier, 1954;
341 Burningham and French, 2014; Hesp et al., 2016). There is no evidence to suggest this is
342 happening at the multiannual time scale (i.e., within last 20 years) as this was not examined
343 in this study, but the generally high energy wave regime, narrow shelf and limited sediment
344 supply may mean that aggradational landforms are quickly ‘flattened’ against the coast (e.g.,
345 Corbella and Stretch, 2012b). Indeed, the forelands identified in this study are generally of
346 greater length and shorter width when compared to those reported elsewhere globally (see for
347 example Sanderson and Eliot, 1996; Klein et al., 2002, for different evolutionary models).

348 This property also has implications for evaluating foreland dynamics (e.g., width/length ratio)
349 and the extent to which the lateral margins of the forelands may be exposed to wave action
350 (Alcántara-Carrió and Fontán, 2009; Xhardé et al., 2011). It is notable that the greatest
351 morphodynamic changes occurring in the forelands examined here are found in association
352 with river mouth/bar locations. Bedrock is clearly imposing a key role in either anchoring or
353 delineating many of the South African forelands which leads to a strong tendency for them to
354 be largely fixed in their alongshore position.

355

356 One significant difference between the cusplate and ramp forelands in this study is that 46%
357 of the former are symmetric in plan view, whereas only 18% of the latter are (Table 1). The
358 reason for this is the rising bedrock surface underlying ramp forelands acts to disrupt
359 longshore transport, leading to differential erosion of the foreland margins and an asymmetric
360 plan form shape (Boeyinga et al., 2010; Vieira da Silva et al., 2018; Gallop et al., 2020).

361 Cusplate forelands, even if they are anchored on a shore platform (as 44 of 46 cusplate
362 forelands in this study area), appear to be better able to operate as headland bypass systems
363 because they retain an active sedimentary foreshore along their entire length (Fig. 7), and this
364 process works through feedback to maintain foreland systems at morphological equilibrium.

365 This may be facilitated by storage of sediment in, and sediment transport to and from,
366 subtidal bars and shoals, in particular around river mouths (Fig. 10). The varied typologies of
367 cusplate to ramp foreland systems, that can be considered to exist along a continuum,
368 highlight the role of bedrock control within the lower shoreface or intertidal zone (Fig. 7).

369 The presence of antecedent bedrock outcrops controls where shoreface pinning will take
370 place, resulting in enhanced erosion of loose sand outside of these areas (Dillenburg et al.,
371 2000; Valvo et al., 2006; Gallop et al., 2020). Over time, therefore, the shoreface becomes
372 more indented and bedrock-influenced forelands develop. This means that macroscale

373 geologic structure can be considered as the major control on foreland development and
374 geometry along sandy coasts. Silveira et al. (2010) describe different styles of sandy coastline
375 response to bedrock outcrops along the coast of Brazil, which they classified as headland-
376 bypassing systems, but this principle works exactly the same for smaller-scale outcrops as
377 described from South Africa in this present study. An interesting point is that, especially
378 along the northeast coast of South Africa, this bedrock influence is commonly provided by
379 aeolianite and, less commonly, by beachrock that may exist across the subtidal to supratidal
380 zones (Miller and Mason, 1994; Knight, 2021). The relief and extent of the bedrock surface
381 largely controls accommodation space on the beach behind.

382

383 In detail, this mechanism of sediment storage in headland bypass systems has been previously
384 described in the literature (Moslow and Heron, 1981; Goodwin et al., 2013; Kumar et al.,
385 2013). Almost all the forelands identified here are contemporary and thus appear to be
386 morphologically active under today's conditions (44 of 87, 50%), or partly active with
387 contemporary geomorphic change taking place in some parts of the system only (42 of 87,
388 48%). All foreland types are also equally split between active and partly active systems. Only
389 one system (Cape Recife, #32) is considered to be largely inactive. This system comprises
390 headland-bypass dunefields that show mid-Holocene stabilised dune ridges overlying earlier
391 coarse beach ridges (Illenberger and Burkinshaw, 2008). These geomorphic elements
392 correspond to the Schelm Hoek Formation, which is of (undifferentiated) late Pleistocene age
393 (Roberts et al., 2014).

394

395 Many of the forelands along the northeast coast of South Africa, and the adjacent coastal
396 plains, are anchored on aeolianite and gravel/sand beach ridges that span MIS 11 to Holocene
397 (Porat and Botha, 2008; Botha et al., 2018). For example, the Cape Vital foreland (#71) is

398 located immediately seaward of Lake Bhangazi that has, at its southern end, a beach berm <6
399 m asl dated by the luminescence method to 1800 ± 160 yr (Botha et al., 2018). Progradational
400 development of the Cape Vital foreland therefore postdates this period. Further, all of these
401 forelands on this northern sector of the KwaZulu-Natal coast (n=15) are the youngest and
402 smallest coastal elements of the Middle to Late Pleistocene coastal aggradational record in
403 this location where the relict coastal plain extends >12 km inland (Sudan et al., 2004; Porat
404 and Botha, 2008). It is also notable that extensive beach ridge sets here are mainly linear,
405 building an aggradational and parallel shoreline rather than a large cusped foreland shoreline
406 (cf., Dungeness: Long and Hughes, 1995; Roberts and Plater, 2007). This may suggest that
407 today's forelands are only reworking sediment along this largely relict coast (Knight, 2021).

408

409 *Forelands and coastal geomorphic systems*

410 The different types of forelands identified in this study have not been described
411 systematically in the literature, and this study is the first to formalise and define these four
412 foreland types (Fig. 1). These different types represent the interplay amongst sediment
413 supply, accommodation space and the presence of bedrock outcrops of different sizes,
414 elevations and locations (Heron et al., 1984; Boeyinga et al., 2010; Goodwin et al., 2013;
415 Vieira da Silva et al., 2018; de Macêdo et al., 2022), and thus these foreland types can be
416 considered to exist along a morphological continuum. This interplay is shown through the
417 development of ramp forelands, where the rise of the bedrock surface towards the foreland
418 apex leads to thinning of the surficial sediment cover which is maintained mainly by
419 supratidal aeolian deposition, with wave-deposited sediments located on the foreland flanks
420 (e.g., at Kaysers Beach (#52) and Rockclyffe-on-Sea (#56)). Ramp forelands therefore also
421 reflect the interplay between wave and wind sediment transport processes that maintain the
422 stability of the foreland as a whole.

423

424 A sediment systems approach can frame the analysis of these relationships (Fig. 10). For
425 example, on the east coast of South Africa, beach recovery after storms takes around two
426 years on average, and is modified by beach–dune interactions (Corbella and Stretch, 2012a,
427 b). This suggests that storms move beach sediment both landward into the dunes and offshore
428 onto the shelf, and that this sediment is then recirculated back to the beach system under
429 fairweather conditions. Along the Eastern Cape coast, Lubke and Webb (2016) described the
430 sediment circulation patterns between the beach–dune system (part of the Boknes Boesman
431 ramp foreland, #35) and the Bushmans River at the north end of this system. Changes in river
432 mouth position from ~1955 onwards led to growth of the beach and dune areas adjacent to
433 the mouth, and this subsequently led (~1970–1980) to new dune areas being stabilised by
434 vegetation in this marginal sector of the foreland. Presently (from ~1997 onwards) dunes are
435 being reactivated at the south end of this system, giving rise to spatial differences along the
436 foreland in sediment availability and supratidal dune dynamics. Along the southern Cape
437 coast, Hellström (1996) showed that changes in the position of the Goukamma River outlet
438 from ~1930 resulted in development of a large ‘spit delta’ which was then naturally
439 vegetated, reducing downdrift sediment supply to the adjacent Buffelskop foreland (#25).

440 Thus, any potential narrowing of this foreland system could be interpreted as a response to
441 this river mouth behaviour. Similar behaviour has also been described adjacent to small rivers
442 flowing into the Río de la Plata estuary, Uruguay (Gutiérrez et al., 2018). These examples
443 illustrate how within-system sediment supply and transport can significantly modify foreland
444 dynamics, independent of direct external forcing. Figure 10 also depicts the main drivers of
445 foreland sediment systems and their dynamical controls. Of note here is that there are
446 functional connections between different landforms within the foreland system that are driven
447 by both wind and water processes. There are also feedbacks between these landforms and

448 therefore the processes that influence them – for example, erosion of vegetated dunes releases
449 more sediment to transverse dunes of the upper beach, building ramp dunes and protecting
450 vegetated dunes inland from further erosion (e.g., He et al., 2022). The present vegetated
451 dunes at the rear of most beaches can be considered as essentially fossilised systems as they
452 are largely not functionally connected to the present beach system (Knight, 2021). Likewise,
453 foreland erosion can also reduce accommodation space for transverse dune development
454 (e.g., at Kaysers Beach, #52). Although there is high variability in dune migration rates
455 within the foreland systems, this appears to be cyclic in behaviour but not strictly seasonal,
456 and there is limited evidence for net alongshore movement of the foreland through dune
457 migration (Knight and Burningham, 2021). The comparison between forelands suggests that
458 at the foreland scale, these systems are actually behaving in a similar fashion. Bigger winter
459 waves, however, may both enhance sediment supply to and increase erosion from the
460 foreland shoreface (Fig. 10), which may be reflected in the geomorphology of foreland
461 margins and, subsequently, on transverse dune geomorphology and sediment supply.
462 Examining foreland sediment budgets is a useful area of future research.

463

464 **Conclusions**

465 This study for the first time identifies four different types of coastal forelands and then
466 inventorises these through a systematic survey of the South African coast. These foreland
467 types are found in different coastal contexts in South Africa, and likely repeated globally, and
468 their distributions and large-scale geomorphic properties illustrate the interplay amongst the
469 different forcing factors that contribute to foreland dynamics, including wind/wave regime
470 and sediment supply. Of the 87 forelands identified across South Africa in this study, 5% are
471 salients, 10% tombolos, 53% cusped and 32% ramp forelands. These have different locations
472 and geomorphic properties, and it is only cusped and ramp forelands that are associated with

473 transverse dunes in their supratidal zones. A sediment systems approach – considering the
474 interplay among fluvial, nearshore, shoreface, supratidal and vegetated dune elements – can
475 usefully inform on foreland sediment budgets and dynamics, and the role of forelands in
476 influencing the dynamics of sandy coasts more generally. The methods presented in this
477 study can be deployed worldwide, and this is a useful research strategy to inform on sandy
478 beach dynamics, with implications for the sensitivity of such beaches to climate forcing.

479

480 **Acknowledgements**

481 We thank two anonymous reviewers for their helpful comments on this paper.

482

483 **References**

- 484 Alcántara-Carrió, J., Fontán, A., 2009. Factors controlling the morphodynamics and
485 geomorphologic evolution of a cusped foreland in a volcanic intraplate island (Maspalomas,
486 Canary Islands). *J Coastal Res* 56, 683–687.
- 487 Allen, T.R., Oertel, G.F., Gares, P.A., 2012. Mapping coastal morphodynamics with
488 geospatial techniques, Cape Henry, Virginia, USA. *Geomorphology* 137, 138–149.
- 489 Ashton, A., Murray, A.B., Arnault, O., 2001. Formation of coastline features by large-scale
490 instabilities induced by high-angle waves. *Nature* 414, 296–300.
- 491 Bate, G.C., Nunes, M., Escott, B., Mnikathi, A., Craigie, J., 2017. Micro-estuary – a new
492 estuary type recognised for South African conditions. *Trans R Soc S Afr* 72, 85–92.
- 493 Black, K.P., Reddy, K.S.K., Kulkarni, K.B., Naik, G.B., Shreekantha, P., Mathew, J., 2020.
494 Salient evolution and coastal protection effectiveness of two large artificial reefs. *J Coastal*
495 *Res* 36, 709–719.

496 Boeyinga, J., Dusseljee, D.W., Pool, A.D., Schoutens, P., Verduin, F., van Zwicht, B.N.M.,
497 Klein, A.H.F., 2010. The effects of a bypass dunefield on the stability of a headland bay
498 beach: A case study. *Coastal Eng* 57, 152–159.

499 Botha, G.A., Porat, N., Haldorsen, S., Duller, G.A.T., Taylor, R., Roberts, H.M., 2018. Beach
500 ridge sets reflect the late Holocene evolution of the St Lucia estuarine lake system, South
501 Africa. *Geomorphology* 318, 112–127.

502 Burningham, H., French, J.R., 2014. Travelling forelands: complexities in drift and migration
503 patterns. *J Coastal Res* SI70, 102–108.

504 Carr, A.S., Bateman, M.D., Cawthra, H.C., Sealy, J., 2019. First evidence for onshore marine
505 isotope stage 3 aeolianite formation on the southern Cape coastline of South Africa. *Mar*
506 *Geol* 407, 1–15.

507 Carter, R.W.G., 1980. Longshore variations in nearshore wave processes at Magilligan Point,
508 Northern Ireland. *Earth Surf Proc* 5, 81–89.

509 Carter, R.W.G., Wilson, P., 1993. Aeolian processes and deposits in northwest Ireland. In:
510 Pye, K. (ed), *The dynamics and environmental context of aeolian sedimentary systems*. *Geol*
511 *Soc Lond, Spec Public* 72, pp. 173–190.

512 Clemmensen, L.B., Bendixen, M., Nielsen, L., Jensen, S., Schrøder, L., 2011. Coastal
513 evolution of a cusped foreland (Flakket, Anholt, Denmark) between 2006 and 2010. *Bull*
514 *Geol Soc Denmark* 59, 37–44.

515 Cooper, J.A.G., 2001. Geomorphological variability among microtidal estuaries from the
516 wave-dominated South African coast. *Geomorphology* 40, 99–122.

517 Corbella, S., Stretch, D.D., 2012a. Decadal trends in beach morphology on the east coast of
518 South Africa and likely causative factors. *Nat Haz Earth Syst Sci* 12, 2515–2527.

519 Corbella, S., Stretch, D.D., 2012b. Shoreline recovery from storms on the east coast of
520 Southern Africa. *Nat Haz Earth Syst Sci* 12, 11–22.

521 Corbella, S., Stretch, D.D., 2012c. The wave climate on the KwaZulu-Natal coast of South
522 Africa. *J S Afr Inst Civil Eng* 54, 45–54.

523 Craig-Smith, S.J., 2005. Cuspate Forelands. In: Schwartz, M.L. (ed), *Encyclopedia of Coastal*
524 *Science*. Springer, Amsterdam, pp. 354–355.

525 Dardis, G.F., Grindley, J.R., 1988. Coastal geomorphology. In: Moon, B.P., Dardis, G.F.
526 (eds), *The Geomorphology of Southern Africa*. Southern Book Publishers, Johannesburg, pp.
527 141–174.

528 de Macêdo, R.J.A., Manso, V.A.V., Klein, A.H.F., 2022. The geometric relationships of
529 salients and tombolos along a mesotidal tropical coast. *Geomorphology* 411, 108311,
530 doi:10.1016/j.geomorph.2022.108311.

531 Dillenburg, S.R., Roy, P.S., Cowell, P.J., Tomazelli, L.J., 2000. Influence of antecedent
532 topography on coastal evolution as tested by the shoreface translation-barrier model (STM). *J*
533 *Coastal Res* 16, 71–81.

534 Dolphin, T.J., Vincent, C.E., Coughlan, C., Rees, J.M., 2007. Variability in sandbank
535 behaviour at decadal and annual time-scales and implications for adjacent beaches. *J Coastal*
536 *Res* SI50, 731–737.

537 Dolphin, T.J., Vincent, C.E., Wihsgott, J., Belhache, M., Bryan, K.R., 2011. Seasonal
538 rotation of a mixed sand-gravel beach. *J Coastal Res* SI64, 65–69.

539 Escoffier, F.F., 1954. Travelling forelands and the shoreline processes associated with them.
540 *Bull US Beach Erosion Board* 9, 11–14.

541 Falqués, A., Kakeh, N., Calvete, D., 2018. A new instability mechanism related to high-angle
542 waves. *Ocean Dyn*, 68, 1169–1179.

543 Fontolan, G., Simeoni, U., 1999. Holocene cuspate forelands in the Strait of Magellan,
544 southern Chile. *Rev Geol Chile* 26, 175–186.

545 Gallop, S.L., Kennedy, D.M., Loureiro, C., Naylor, L.A., Muñoz-Pérez, J.J., Jackson,
546 D.W.T., Fellowes, T.E., 2020. Geologically controlled sandy beaches: Their geomorphology,
547 morphodynamics and classification. *Science of the Total Environment* 731, 139123,
548 doi:10.1016/j.scitotenv.2020.139123.

549 Goodwin, I.D., Freeman, R., Blackmore, K., 2013. An insight into headland sand bypassing
550 and wave climate variability from shoreface bathymetric change at Byron Bay, New South
551 Wales, Australia. *Mar Geol* 341, 29–45.

552 Green, A.N., Pillay, T., Cooper, J.A.G., Guisado-Pintado, E., 2019. Overwash-dominated
553 stratigraphy of barriers with intermittent inlets. *Earth Surf Proc Landf* 44, 2097–2111.

554 Guastella, L.A., Smith, A.M., 2014. Coastal dynamics on a soft coastline from serendipitous
555 webcams: KwaZulu-Natal, South Africa. *Estuar Coastal Shelf Sci* 150, 76–85.

556 Gulliver, F.P., 1896. Cuspate forelands. *Bull Geol Soc Am* 7, 899–422.

557 Gutiérrez, O., Panario, D., Nagy, G.J., 2018. Relationships between the sand cycle and the
558 behaviour of small river mouths: a neglected process. *J Sediment Env* 2, 307–325.

559 Hammer, Ø., Harper, D.A.T., Ryan, P.D., 2001. PAST: paleontological statistics software
560 package for education and data analysis. *Palaeontol Electr* 4, 4, [http://palaeo-](http://palaeo-electronica.org/2001_1/past/issue1_01.htm)
561 [electronica.org/2001_1/past/issue1_01.htm](http://palaeo-electronica.org/2001_1/past/issue1_01.htm)

562 Harris, L., Nel, R., Schoeman, D., 2011. Mapping beach morphodynamics remotely: A novel
563 application tested on South African sandy shores. *Estuar Coastal Shelf Sci* 92, 78–89.

564 He, Y., Liu, J., Cai, F., Li, B., Qi, H., Zhao, S., 2022. Aeolian sand transport influenced by
565 tide and beachface morphology. *Geomorphology* 396, 107987,
566 doi:10.1016/j.geomorph.2021.107987.

567 Hellström, G.B., 1996. Preliminary investigations into recent changes of the Goukamma
568 Nature Reserve frontal dune system, South Africa – with management implications. *Landsc*
569 *Urban Plann* 34, 225–235.

570 Hellström, G.B., Lubke, R.A., 1993. Recent Changes to a Climbing-Falling Dune System on
571 the Robberg Peninsula Southern Cape Coast, South Africa. *J Coastal Res* 9, 647–653.

572 Heron Jr, S.D., Moslow, T.F., Berelson, W.M., Herbert, J.R., Steele III, G.A., Susman, K.R.,
573 1984. Holocene sedimentation of a wave-dominated barrier-island shoreline: Cape Lookout,
574 North Carolina. *Mar Geol* 60, 413–434.

575 Hesp, P.A., Ruz, M.-H., Hequette, A., Marin, D., Miot da Silva, G., 2016. Geomorphology
576 and dynamics of a traveling cusped foreland, Authie estuary, France. *Geomorphology* 254,
577 104–120.

578 Hunter, R.E., Richmond, B.M., Alpha, T.R., 1983. Storm-controlled oblique dunes of the
579 Oregon coast. *Geol Soc Am Bull* 94, 1450–1465.

580 Illenberger, W.K., Burkinshaw, J.R., 2008. Coastal dunes and dunefields. In: Lewis, C.A.
581 (ed), *Geomorphology of the Eastern Cape*. NISC, Grahamstown, pp. 85–106.

582 Jackson, D.W.T., Cooper, A., Green, A., Beyers, M., Guisado-Pintado, E., Wiles, E.,
583 Benallack, K., Balme, M., 2020. Reversing transverse dunes: Modelling of airflow switching
584 using 3D computational fluid dynamics. *Earth Planet Sci Lett* 544, 116363,
585 doi:10.1016/j.epsl.2020.116363.

586 Klein, A.H.F., Andriani Jr, N., de Menezes, J.T., 2002. Shoreline salients and tombolos on
587 the Santa Catarina coast (Brazil): description and analysis of the morphological relationships.
588 *J Coastal Res* SI36, 425–440.

589 Knight, J., 2021. The late Quaternary stratigraphy of coastal dunes and associated deposits in
590 South Africa. *S Afr J Geol* 124, 995–1006.

591 Knight, J., Burningham, H., 2019. Sand dunes and ventifacts on the coast of South Africa.
592 *Aeolian Res* 37, 44–58.

593 Knight, J., Burningham, H., 2021. The morphodynamics of transverse dunes on the coast of
594 South Africa. *Geo-Mar Lett* 41, 47, doi:10.1007/s00367-021-00717-4.

595 Knight, J., Harrison, S., 2009. Sediments and future climate. *Nat Geosci* 3, 230.

596 Kumar, N., Voulgaris, G., List, J.H., Warner, J.C., 2013. Alongshore momentum balance
597 analysis on a cusped foreland. *J Geophys Res: Oceans* 118, 5280–5295.

598 Kunte, P.D., Wagle, B.G., 1993. Determination of Net Shore Drift Direction of Central West
599 Coast of India Using Remotely Sensed Data. *J Coastal Res* 9, 811–822.

600 La Cock, G.D., Lubke, R.A., Wilken, M., 1992. Dune movement in the Kwaihoek region of
601 the Eastern Cape, South Africa, and its bearing on future developments of the region. *J*
602 *Coastal Res* 8, 210–217.

603 Lampe, M., Lampe, R., 2018. Evolution of a large Baltic beach ridge plain (Neudarss, NE
604 Germany): A continuous record of sea-level and wind-field variation since the Homeric
605 Minimum. *Earth Surf Proc Landf* 43, 3042–3056.

606 Long, A.J., Hughes, P.D.M., 1995. Mid- and late-Holocene evolution of the Dungeness
607 foreland, UK. *Mar Geol* 124, 253–271.

608 Lubke, R.A., Webb, C., 2016. The interaction between the dunes system and the lower
609 estuary at the Bushmans River Mouth, Eastern Cape over the past 60 years. *S Afr J Bot* 107,
610 148–159.

611 Luijendijk, A., Hagenars, G., Ranasinghe, R., Baart, F., Donchyts, G., Aarninkhof, S., 2018.
612 The State of the World's Beaches. *Sci Rept* 8, 6641, doi:10.1038/s41598-018-24630-6.

613 McNinch, J.E., Luettich Jr, R.A., 2000. Physical processes around a cusped foreland:
614 implications to the evolution and long-term maintenance of a cape-associated shoal. *Cont*
615 *Shelf Res* 20, 2367–2389.

616 Meeuwis, J., van Rensburg, P.A.J., 1986. Logarithmic spiral coastlines: the northern Zululand
617 coast. *S Afr Geogr J* 68, 18–44.

618 Miller, W.R., Mason, T.R., 1994. Erosional features of coastal beachrock and aeolianite
619 outcrops in Natal and Zululand, South Africa. *J Coastal Res* 10, 374–394.

620 Mitchell, J., Jury, M.R., Mulder, G.J., 2005. A study of Maputaland beach dynamics. *S Afr*
621 *Geogr J* 87, 43–51.

622 Moslow, T.F., Heron Jr, S.D., 1981. Holocene depositional history of a microtidal cusped
623 foreland cape: Cape Lookout, North Carolina. *Mar Geol* 41, 251–270.

624 Nordstrom, K.F., Terich, T.A., 1986. Management considerations for accreting shorelines.
625 *Coastal Zone Manage J* 13, 131–150.

626 Olivier, M.J., Garland, G.G., 2003. Short-term monitoring of foredune formation on the east
627 coast of South Africa. *Earth Surf Proc Landf* 28, 1143–1155.

628 Orlando, L., Ortega, L., Defeo, O., 2019. Multi-decadal variability in sandy beach area and
629 the role of climate forcing. *Estuar Coastal Shelf Sci* 218, 197–203.

630 Park, J.-Y., Wells, J.T., 2005. Longshore transport at Cape Lookout, North Carolina: shoal
631 evolution and the regional sediment budget. *J Coastal Res* 21, 1–17.

632 Park, J.-Y., Wells, J.T., 2007. Spit growth and downdrift erosion: Results of longshore
633 transport modeling and morphologic analysis at the Cape Lookout cusped foreland. *J Coastal*
634 *Res* 23, 553–568.

635 Porat, N., Botha, G., 2008. The luminescence chronology of dune development on the
636 Maputaland coastal plain, southeast Africa. *Quat Sci Rev* 27, 1024–1046.

637 Rautenbach, C., Barnes, M.A., de Vos, M., 2019. Tidal characteristics of South Africa. *Deep-*
638 *Sea Res Part I* 150, 103079, doi.org/10.1016/j.dsr.2019.103079.

639 Roberts, H.M., Plater, A.J., 2007. Reconstruction of Holocene foreland progradation using
640 optically stimulated luminescence (OSL) dating: an example from Dungeness, UK. *Holocene*
641 17, 495–505.

642 Roberts, D., Cawthra, H., Musekiwa, C., 2014. Dynamics of late Cenozoic aeolian deposition
643 along the South African coast: a record of evolving climate and ecosystems. In: Martini, I.P.,

644 Wanless, H.R. (eds), *Sedimentary Coastal Zones from High to Low Latitudes: Similarities*
645 *and Differences*. Geol Soc Lond, Spec Public 388, pp. 353–387.

646 Sanderson, P.G., Eliot, I., 1996. Shoreline salients, cusped forelands and tombolos on the
647 Coast Australia. *J Coastal Res* 12, 761–773.

648 Sanderson, P.G., Eliot, I., Hegge, B., Maxwell, S., 2000. Regional variation of coastal
649 morphology in southwestern Australia: a synthesis. *Geomorphology* 34, 73–88.

650 Schumann, E.H., Martin, J.A., 1991. Climatological aspects of the coastal wind field at Cape
651 Town, Port Elizabeth and Durban. *S Afr Geogr J* 73, 48–51.

652 Searson, S., 1994. Extreme sea levels around the coast of southern Africa. Unpublished MSc
653 dissertation, University of Cape Town, 101pp.

654 Semeniuk, V., Searle, D.J., Woods, P.J., 1988. The sedimentology and stratigraphy of a
655 cusped foreland, southwestern Australia. *J Coastal Res* 4, 551–564.

656 Silveira, L.F., Klein, A.H.F., Tessler, M.G., 2010. Headland-bay beach planform stability of
657 Santa Catarina State and of the northern coast of São Paulo State. *Braz J Oceanogr* 58, 101–
658 122.

659 St-Hilaire-Gravel, D., Forbes, D.L., Bell, T., 2015. Evolution and morphodynamics of a
660 prograded beach-ridge foreland, northern Baffin Island, Canadian Arctic archipelago. *Geogr*
661 *Ann: Ser A, Phys Geogr* 97, 615–631.

662 Sudan, P., Whitmore, G., Uken, R., Woodbourn, S., 2004. Quaternary evolution of the coastal
663 dunes between Lake Hlabane and Cape St Lucia, KwaZulu-Natal. *S Afr J Geol* 107, 355–
664 376.

665 Tinley, K.L., 1985. *Coastal Dunes of South Africa*. CSIR, Pretoria, 300pp.

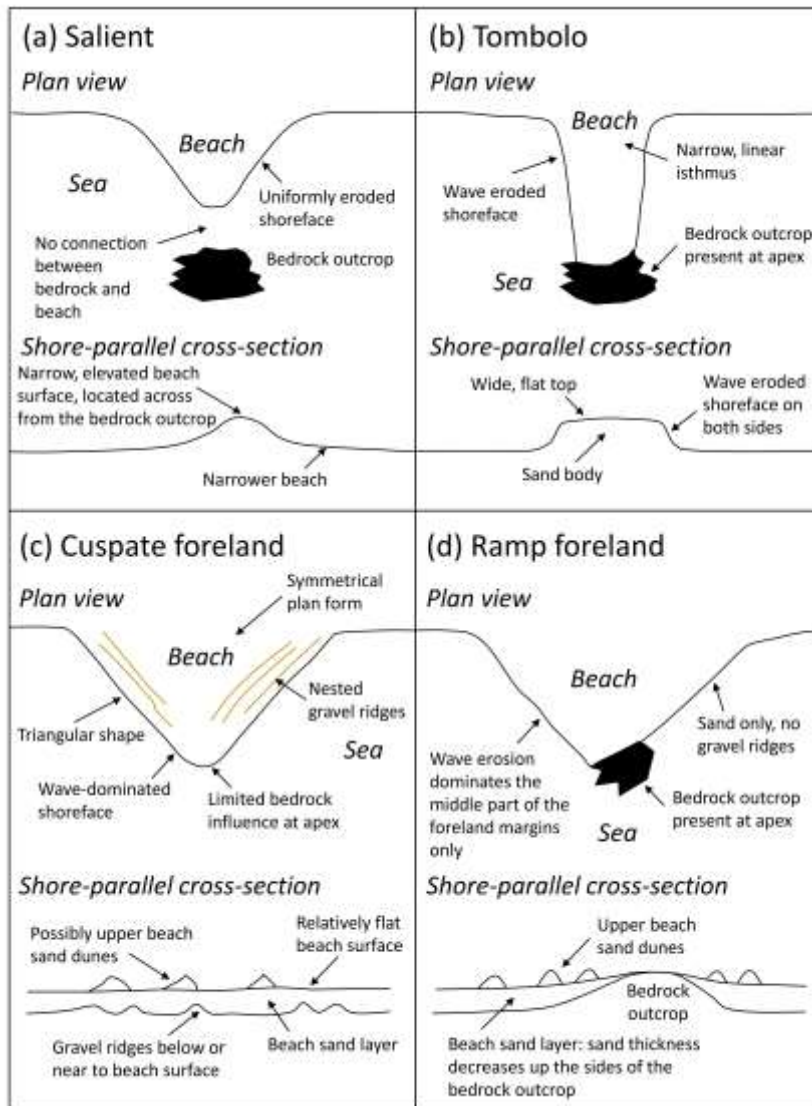
666 Valvo, L.M., Murray, A.B., Ashton, A., 2006. How does underlying geology affect coastline
667 change? An initial modeling investigation. *J Geophys Res* 111, F02025,
668 doi:10.1029/2005JF000340.

669 Veitch, J., Rautenbach, C., Hermes, J., Reason, C., 2019. The Cape Point wave record,
670 extreme events and the role of large-scale modes of climate variability. *J Marine Syst* 198,
671 103185, doi:10.1016/j.jmarsys.2019.103185.

672 Vieira da Silva, G., Toldo Jr, E.E., Klein, A.H.F., Short, A.D., 2018. The influence of wave-,
673 wind- and tide-forced currents on headland sand bypassing – Study case: Santa Catarina
674 Island north shore, Brazil. *Geomorphology* 312, 1–11.

675 Wepener, V., Degger, N., 2019. South Africa. In: Sheppard, C. (ed), *World Seas: an*
676 *Environmental Evaluation*, 2nd Ed. Volume II: the Indian Ocean to the Pacific. Elsevier,
677 Amsterdam, pp. 101–119.

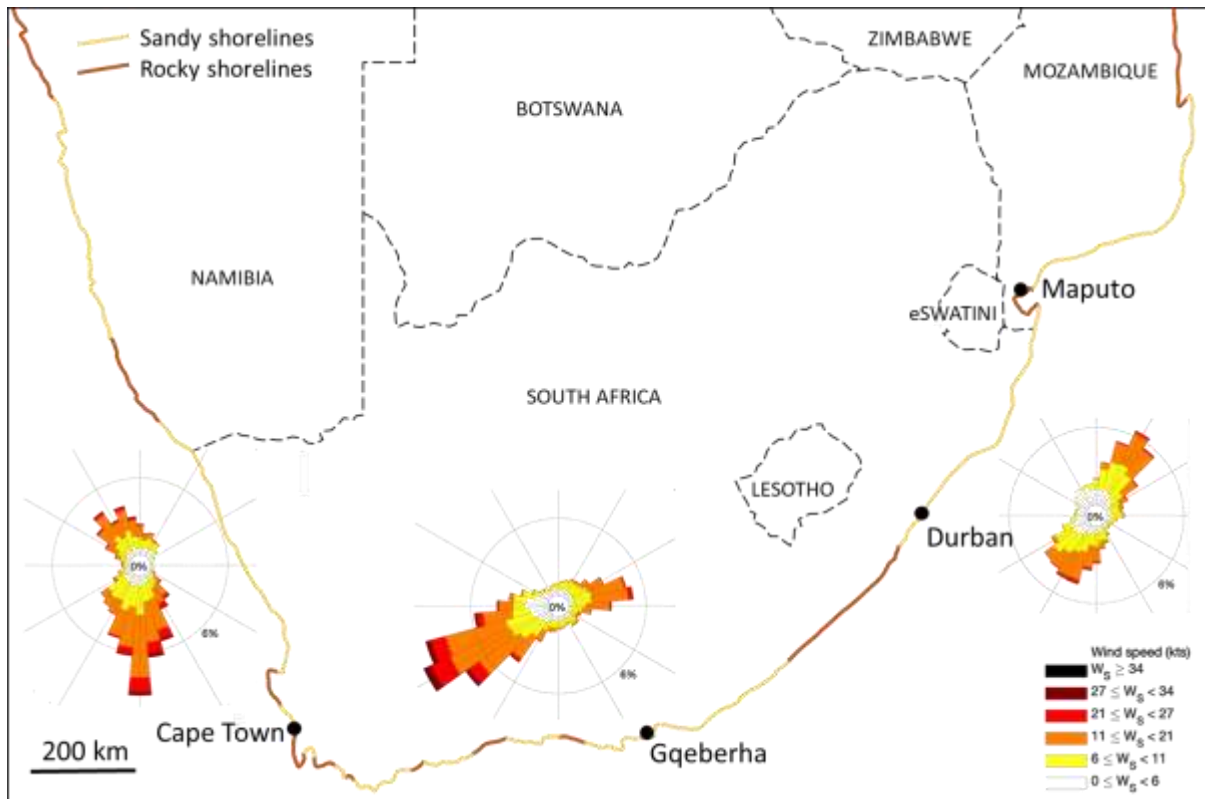
678 Xhardé, R., Long, B.F., Forbes, D.L., 2011. Short-term beach and shoreface evolution on a
679 cusped foreland observed with airborne topographic and bathymetric LIDAR. *J Coastal Res*
680 *SI62*, 50–61.



681

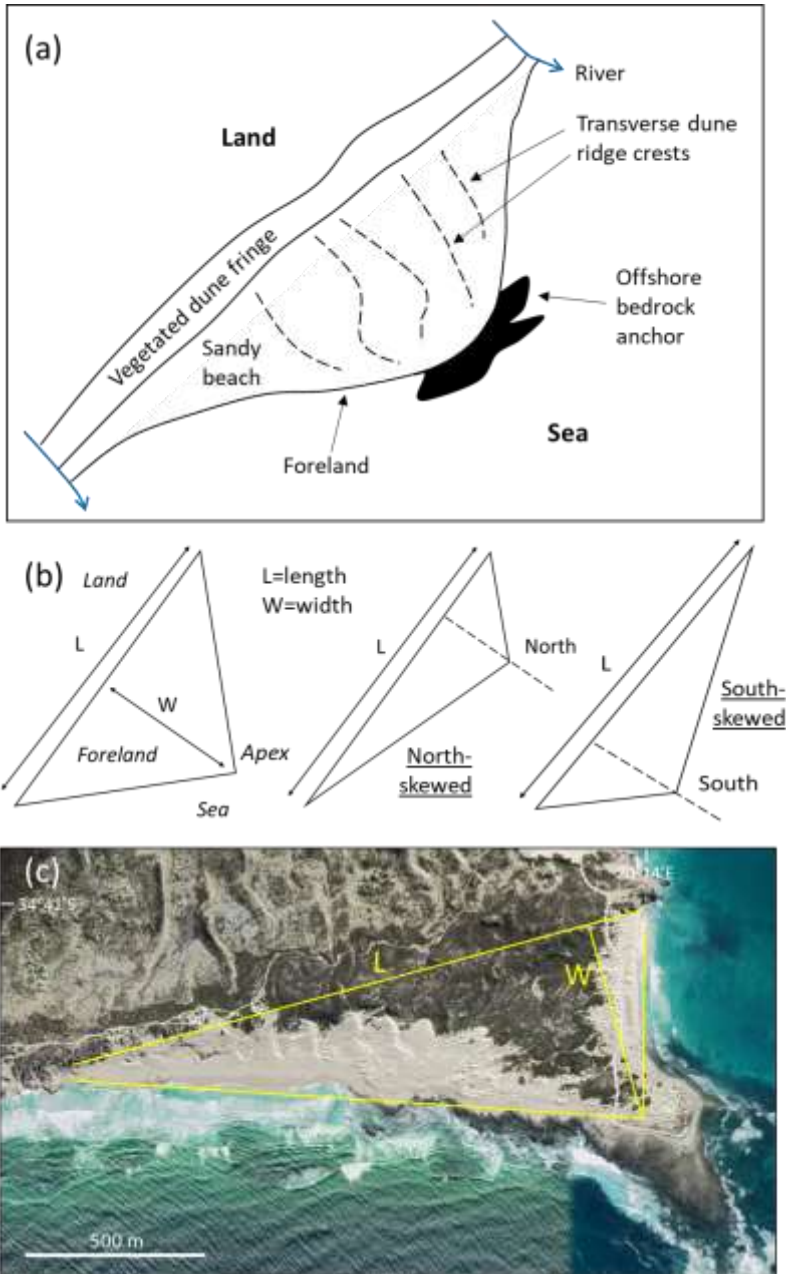
682 Figure 1. Schematic illustration of coastal foreland types and their major morphology

683 properties. Schematic shore-parallel cross-sections are not to scale.



684

685 Figure 2. Map of southern Africa showing the broad differentiation between sandy and rock
 686 shorelines (after Tinley, 1985; Dardis and Grindley, 1988). Illustrative wind roses for the
 687 west coast (Cape Town, 1975 to 2020), south coast (Port Elizabeth, 2001 to 2020) and east
 688 coast (Durban, 1975 to 2020) are also shown.



689

690 Figure 3. (a) Sketch of the main geomorphic elements of a coastal foreland, (b) schematic
 691 view of (top) foreland length and width, as measured in this study, and (bottom) asymmetry
 692 or skewness of the foreland shape where the position of the greatest width is skewed to the
 693 north or south part of the foreland, (c) example of morphometric analysis from Arniston
 694 foreland (#24).

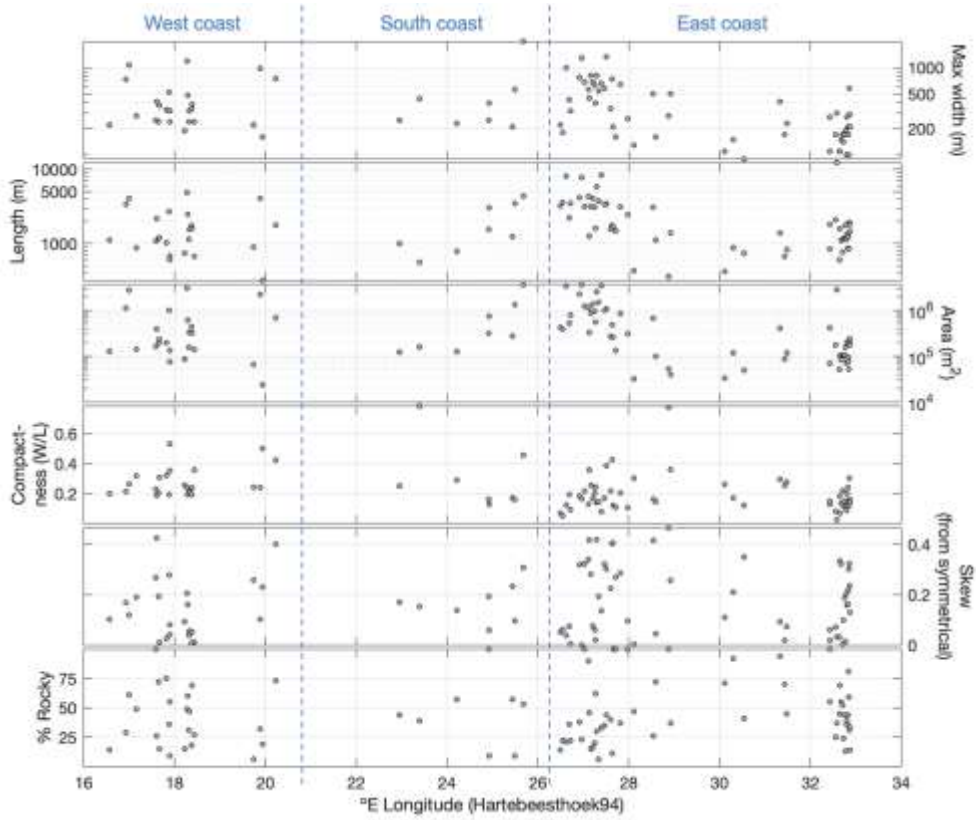


695

696 Figure 4. Map of the South African coast showing the position of coastal forelands identified
 697 in this study using Google Earth imagery. Numbered forelands 1–87 classified into the four
 698 different foreland types are listed in Table 1.

699

700

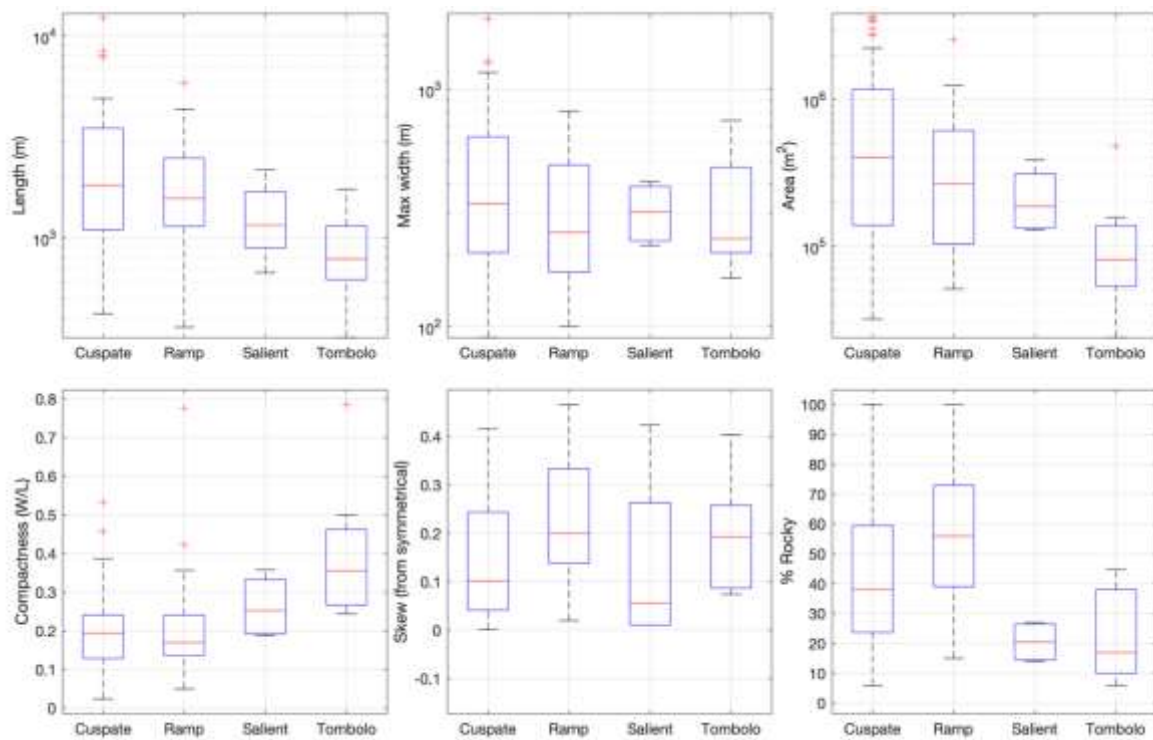


701

702 Figure 5. Plot of longshore (from west to east) variations in foreland morphometric properties
703 along the South African coast.

704

705



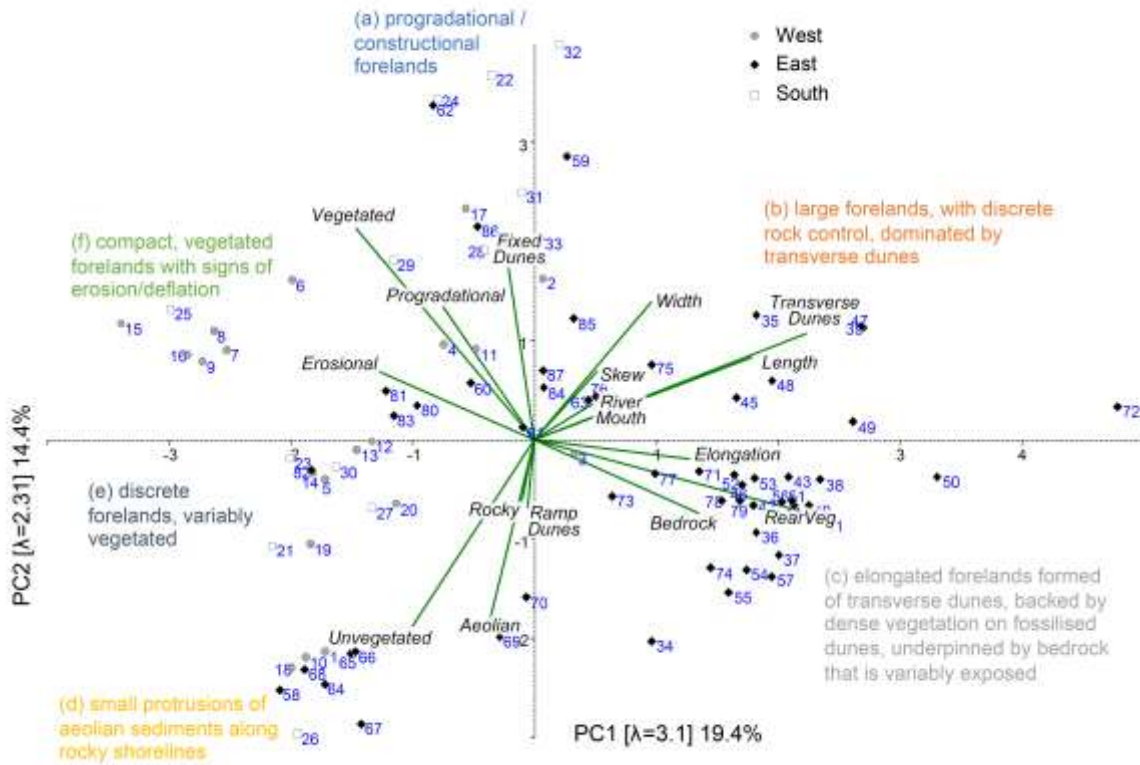
706

707 Figure 6. Examination of key foreland properties: length, width at the apex,
708 compactness (width/length), skewness (from symmetrical), and proportion of the foreland
709 shoreline comprising bedrock.

710



711
 712 Figure 7. Examples of different foreland types along the South African coast. (a) Salient
 713 foreland (#1 Visagiesfontein), (b) tombolo foreland (#26 Robberg), (c) cusped foreland (#39
 714 Oceana Beach), (d) ramp foreland (#42 Fort D'Acre). Locations are marked on Figure 4.
 715

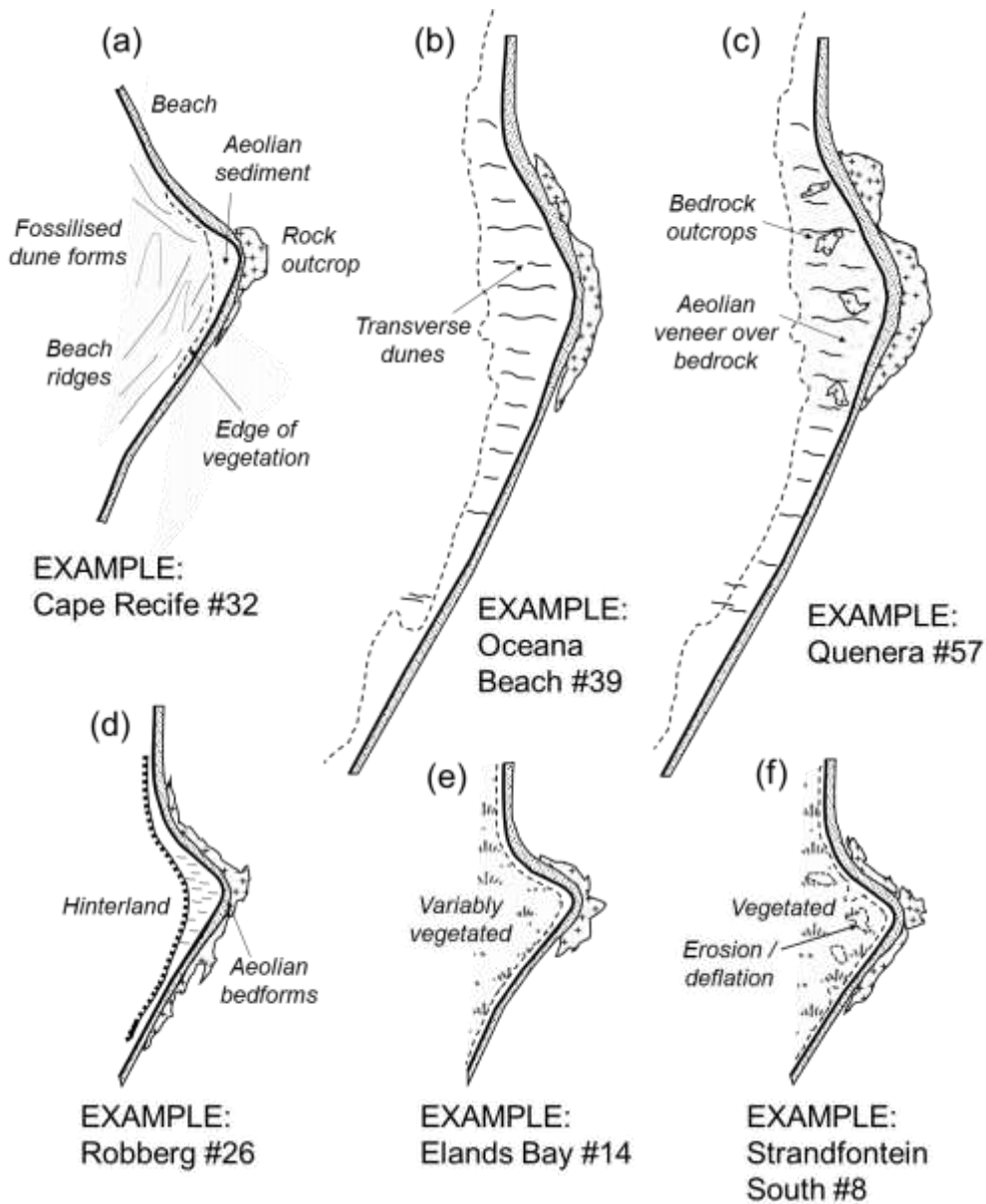


716

717

718 Figure 8. PCA results based on foreland morphometric and geomorphic properties from the
 719 South African coast, from which six endmembers (a–f) are identified (shown in Fig. 9). The
 720 morphometrics shown in Figures 5 and 6, except for area (as it correlates strongly with
 721 length), are used in addition the pseudo (binary) variables representing presence / absence of
 722 different properties and features: river mouth, transverse dunes, fixed dunes, ramp dunes,
 723 exposed bedrock, deflation zone, contemporary progradational forms, distinct aeolian
 724 bedforms, vegetation present on the foreland, vegetation only present at the rear (mainland),
 725 and unvegetated forelands.

726

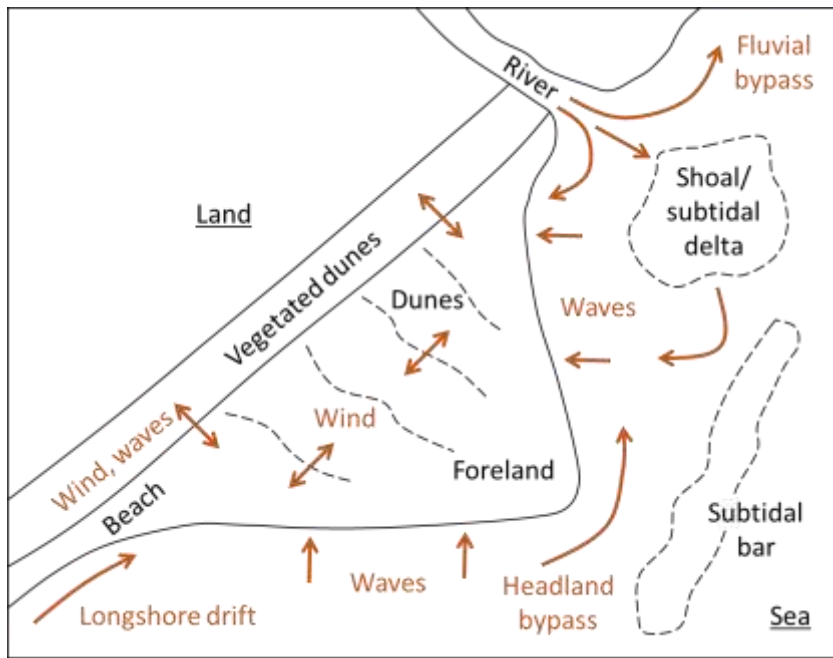


727

728

729 Figure 9. Sketches of the major geomorphic characteristics of the six endmembers identified
730 by PCA analysis of foreland morphometric and geomorphic properties.

731



732

733

734 Figure 10. Schematic representation of physical processes (brown text) leading to sediment

735 transport within a coastal foreland system (brown arrows).

736

737

738

739 Table 1. List of forelands identified along the coast of South Africa (numbered in Figure 4)

740 and their major geomorphic properties.

741

742 Supplementary Data File. Google Earth kzm file of the locations of the forelands examined in

743 this study.